Available online at www.sciencedirect.com
ScienceDirect
Journal of Photochemistry and Photobiology A: Chemistry 183 (2006) 70–78
Journal of Photochemistry and Photobiology A:Chemistry
www.elsevier.com/locate/jphotochem

NMR and kinetic investigations of the multistep photochromism of 3-thienyl-naphthopyrans

D. Venec [a], S. Delbaere [a,*], J.C. Micheau [b], M. Frigoli [c],
C. Moustrou [c], A. Samat [c], G. Vermeersch [a]

[a] CNRS UMR 8009, Université de Lille 2, Faculté de Pharmacie, F-59006 Lille Cedex, France
[b] CNRS UMR 5623, Université Paul Sabatier, IMRCP, Toulouse F-31062, France
[c] CNRS UMR 6114, Université de la Méditerranée, Faculté des Sciences de Luminy, 13288 Marseille Cedex 9, France

Received 31 January 2006; received in revised form 17 February 2006; accepted 20 February 2006

Abstract

The photocolouration under UV irradiation and the thermal relaxation after irradiation of 3-phenyl-3H-naphtho[2,1-b]pyrans linked to one, two, or three thiophene units in 3 position of the pyran moiety have been investigated by NMR. The characterization of each of the four transoid photomerocyanines, as well as the kinetic parameters of photochemical and thermal reactions were obtained and discussed.

Keywords: Photochromism; Kinetics analysis; NMR spectroscopy

1. Introduction

In the course of developing novel photochromic molecules, 3H-naphtho[2,1-b]pyrans bearing thienyl groups have been synthesised [1–3]. The purpose of the electron-rich thienyl substituent was the exploration of the possibility to obtain photoactivable organic conductors or semiconductors [4–11]. These compounds have been investigated either by femtosecond and nanosecond [12] or by conventional absorption spectroscopy [13,14] and more recently, NMR spectroscopy has been used to study the structural and photokinetic properties of some thienyl photochromic derivatives [15,16] including naphthopyrans [17–19]. The NMR spectral resolution brings the considerable advantage to characterise each accumulated photoisomer and to provide the opportunity of the accurate monitoring of their time-evolution under irradiation or in the dark. This is of the highest interest if both a structural investigation and a comprehensive kinetic analysis of a complex photochromic system are considered [20–22]. The photoinduced C–O bond cleavage of the 3-thienyl-naphthopyrans leads to four transoid photomerocyanines isomers under continuous irradiation (Scheme 1). We report here the structural identification and the kinetic analysis of the five-isomer systems that have been observed during the photochromism of the 3-thienyl-naphthopyrans NP1 (R = Th), NP2 (R = Th_2) and NP3 (R = Th_3). The effect of the number of thienyl units on the kinetic parameters of the photochemical and thermal isomerization processes is discussed.

2. Experimental

2.1. Materials

The compounds have previously been synthesised [23].

2.2. NMR investigations and experimental conditions

Thermostated samples (concentration between 6.10^{-3} and 10^{-2} M in toluene-d_8) were irradiated directly in the NMR tube (5 mm), using a 1000 W Xe–Hg HP filtered (Schott 011FG09, 259 nm < λ < 388 nm) short-arc lamp (Oriel). After irradiation, the sample was rapidly transferred into the thermoregulated probe of a Bruker Avance-DPX NMR spectrometer (^1H, 300 MHz).

---

[*] Corresponding author. Tel.: +33 3 20 964 013.
E-mail address: stephanie.delbaere@univ-lille2.fr (S. Delbaere).

1010-6030/$ – see front matter © 2006 Elsevier B.V. All rights reserved.
doi:10.1016/j.jphotochem.2006.02.023

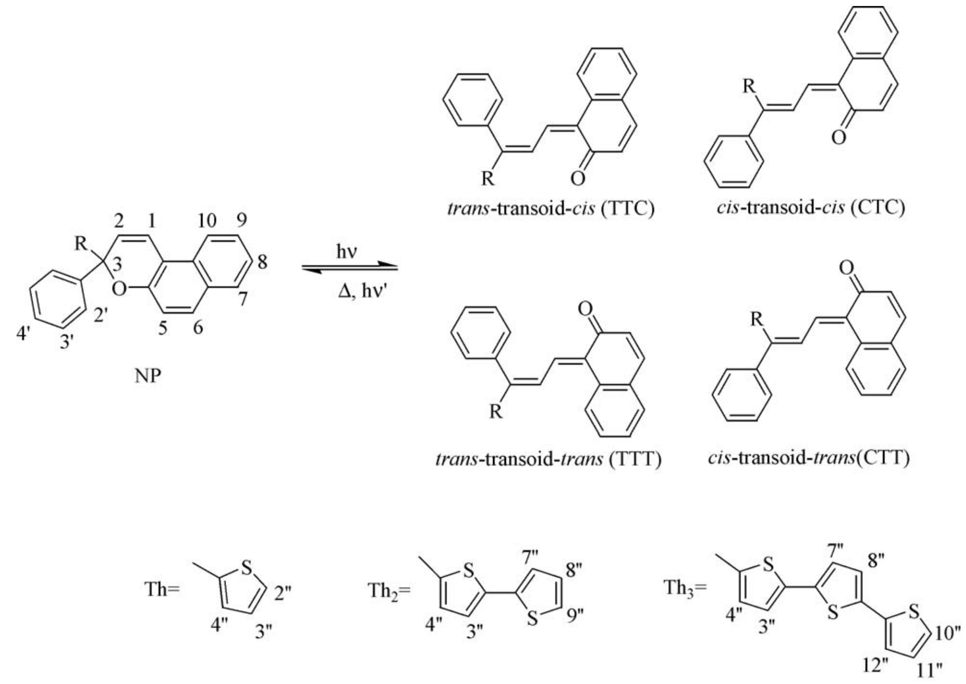

Compound	NP1	NP2	NP3
R	-Th	$-Th_2$	$-Th_3$

Scheme 1. Photochromic equilibrium and corresponding structures of the various 3-thienyl-naphthopyran isomers.

2.3. Data analysis

The calculated concentration evolution was obtained by numerical integration of the set of differential equations written from a five-species system (Scheme 2) using homemade curve fitting software [24].

Assuming that the rate equations corresponding to Scheme 2 are first-order [25], the following set of coupled differential equations is derived.

$$\begin{aligned} \mathrm{d}[0]/\mathrm{d}t &= -(v_{01}+v_{02}+v_{03}+v_{04)}[0]+v_{10}[1]+v_{20}[2] \\ &\quad +v_{30}[3]+v_{40}[4]; \end{aligned}$$

$$\mathrm{d}[1]/\mathrm{d}t = -(v_{10}+v_{12}+v_{14})[1]+v_{01}[0]+v_{21}[2]+v_{41}[4];$$

$$\mathrm{d}[2]/\mathrm{d}t = -(v_{20}+v_{21}+v_{23})[2]+v_{02}[0]+v_{12}[1]+v_{32}[3];$$

$$\mathrm{d}[3]/\mathrm{d}t = -(v_{30}+v_{32}+v_{34})[3]+v_{03}[0]+v_{23}[2]+v_{43}[4];$$

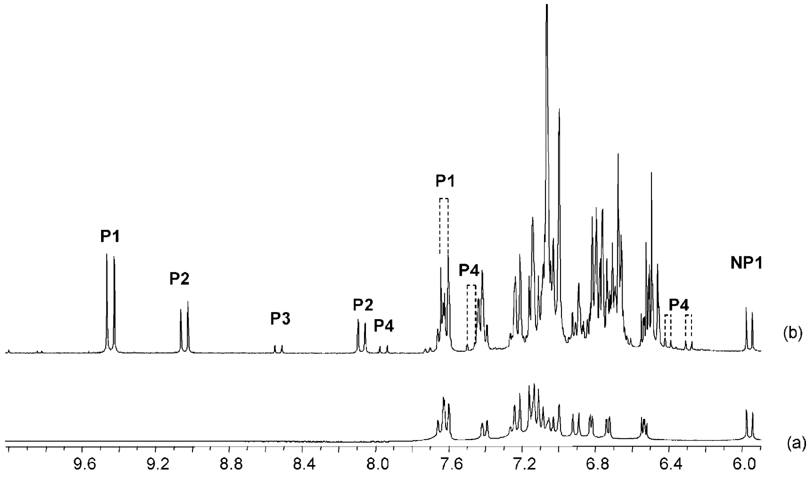

Fig. 1. ^{1}H NMR spectra of NP1 (a) before and (b) after 20 min of UV irradiation at 213 K.

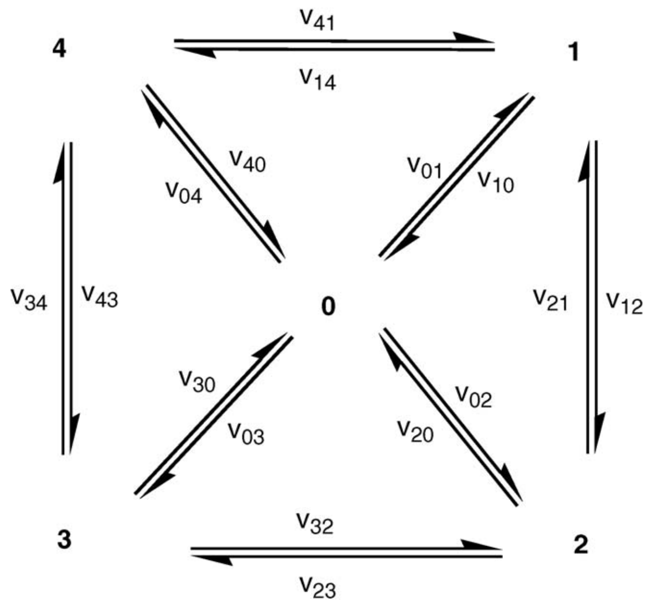

Scheme 2. Possible one-step isomerization paths between the five isomers (0 = initial closed form; 1–4 = photomerocyanines). Two-step isomerizations (for instance between CTC and TTT or between TTC and CTT) are not considered.

$$d[4]/dt = -(v_{40} + v_{41} + v_{43})[4] + v_{04}[0] + v_{14}[1] + v_{34}[3];$$

with $v_{ij} = \Phi_{ij}\varepsilon_i l I_0 F + k_{ij}$.

Φ_{ij} is the quantum yield of the photochemical transformation of compound "X_i" into compound "X_j", ε_i the molar absorption coefficient of compound X_i at the irradiation wavelength, l the optical path, I_0 the incident photon flux, F the photokinetic factor and k_{ij} the rate constant of the thermal transformation of compound "X_i" into compound "X_j".

We have found that the fitting procedure was very selective among the various possible processes taken into consideration. For instance, the simulated kinetic curves were significantly distant from their corresponding experimental data if some important pathway was omitted or if the presence of a forbidden process was artificially imposed [26].

3. Results and discussion

3.1. Structural identification of photoproducts

UV irradiation led to the appearance of several signals with different peak intensities as illustrated in the ^{1}H NMR spectra of NP1 in Fig. 1. These signals fully disappeared during thermal evolution in the dark, then characterizing the formation of metastable photomerocyanines.

Two doublet signals are distinguished at 9.52 ppm ($^3J = 12.1$ Hz) (P1) and at 9.09 ppm ($^3J = 11.8$ Hz) (P2). The measured values of coupling constant and the downfield chemical shifts make it possible to attribute these signals to protons H2 (deshielded by C=O) in transoid–cis type compounds (TTC and CTC) [27]. Two other signals with $^3J = 11.2$ Hz, with low intensity at 8.54 and 7.97 ppm (P3 and P4) are also observed. 2D ^{1}H–^{1}H cosy NMR experiment (Fig. 2) underlined the H_2–H_1 spin–spin coupling for all of the four photomerocyanines: (P1) 9.52 and 7.65 ppm; (P2) 9.09 and 8.09 ppm; (P3) 8.54 and 7.04 ppm; and (P4) 7.97 and 7.45 ppm. Careful examination of peak intensities and coupling constants in 1D spectrum and scalar correlations in 2D-cosy made it possible to identify protons of the major-concentrated compound, P1. $H_{3''}$ at 6.47 ppm ($^3J = 5.0$ and 3.9 Hz) is correlated with protons $H_{2''}$ and $H_{4''}$ ($^4J = 1.1$ Hz) at 6.73 and 6.57 ppm, respectively. Two doublet signals at 6.52 and 6.61 ppm with $^3J = 9.52$ Hz, are assigned to protons H_5 and H_6. A system of four coupled protons is also observed at 6.65 and 7.21 ppm (H_9 and H_{10}) and 6.78 and 6.87 ppm (H_7 and H_8). For the second isomer P2, the doublet of doublet signal at 6.74 ppm is attributed to proton $H_{2''}$ and signals at 7.41 and 7.00 ppm to protons $H_{2'}$ and $H_{3'}$, respectively.

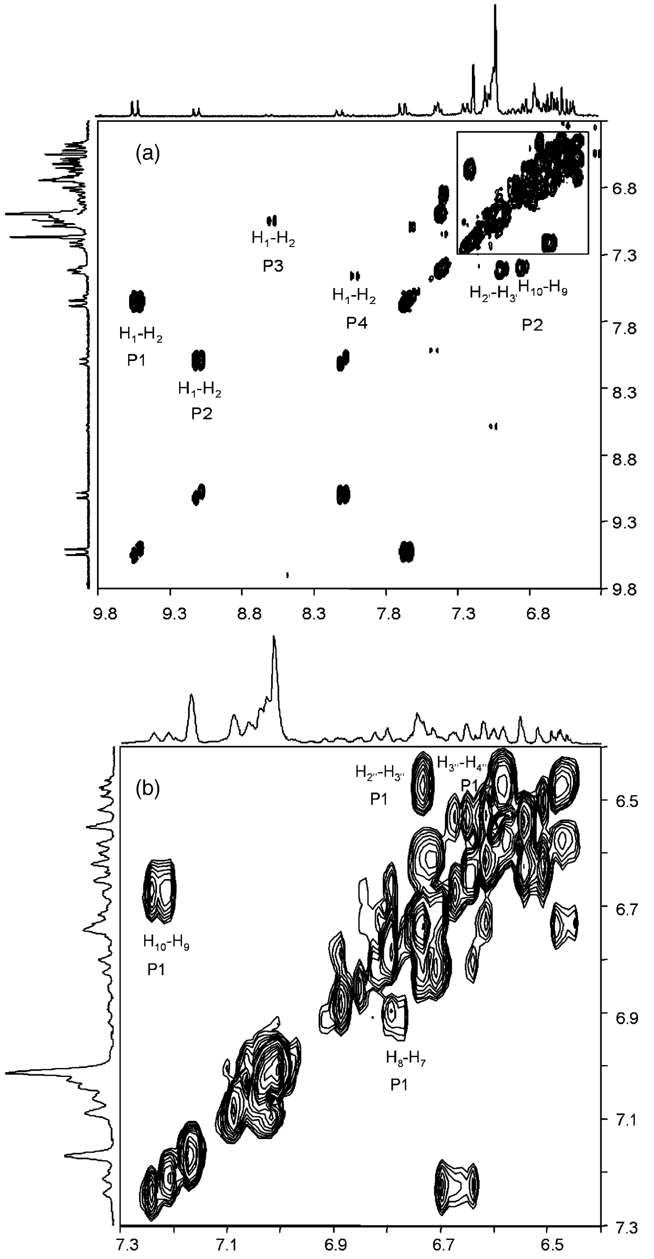

Fig. 2. ^{1}H NMR cosy of NP1 after 20 min of UV irradiation at 213 K: (a) general spectrum and (b) magnification of the inset.

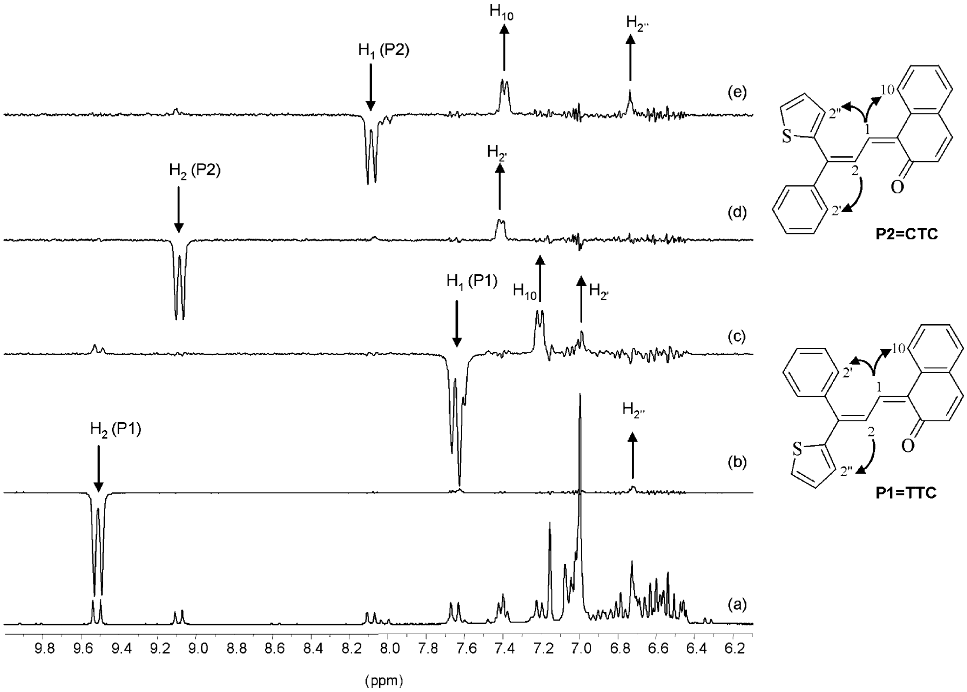

Fig. 3. ^{1}H NMR roesy 1D spectra of NP1 (a) after 20 min of UV irradiation at 213 K; (b) saturation of P1, H_2 doublet at 9.52 ppm showing the exaltation of $H_{2''}$; (c) saturation of P1, H_1 doublet at 7.65 ppm showing the exaltation of H_{10} and $H_{2'}$; (d) saturation of P2, H_2 doublet at 9.09 ppm showing the exaltation of $H_{2'}$; and (e) saturation of P2, H_1 doublet at 8.09 ppm showing the exaltation of H_{10} and $H_{2''}$. The structures P2 = CTC and P1 = TTC show the specific dipolar contacts.

The exact isomery has been proved by recording 1D-roesy experiments. By saturating the doublet signal of P1 at 9.52 ppm, H_2 (Fig. 3b), dipolar effect is measured on proton at 6.73 ppm, assigned to $H_{2''}$ in P1. Another dipolar coupling is also observed between signal at 7.65 ppm (H_1) and protons at 7.21 and 7.01 ppm, then assigned to H_{10} and $H_{2'}$, respectively (Fig. 3c).

The saturation of doublet of P2 at 9.09 ppm (H_2) gives rise to exaltation of signal at 7.41 ppm (Fig. 3d), and that of signal at 8.09 ppm (H_1) to exaltation of resonances at 7.39 (H_{10}) and 6.74 ($H_{2''}$) ppm (Fig. 3e). Such dipolar contacts are consistent with P1 = TTC and P2 = CTC isomery.

The exact isomery of the two last isomers, P3 and P4 is difficult to obtain due to the low peak intensity of their signals. Nevertheless, the signals at 8.54 and 7.97 ppm have been attributed to protons H_1 in P3 = CTT and P4 = TTT, respectively. This attribution has been made by comparing chemical shifts and electronic environment of these two protons with those of protons H_2 in TTC and CTC. Indeed, the proximity of thienyl group leads to a more deshielding shift. This assumption has

Table 1
^{1}H NMR chemical shifts (in ppm) of photomerocyanines obtained from 3-thienyl naphthopyrans NP1, NP2 and NP3

	Chemical shifts/ppm											
	TTC1	CTC1	TTT1	CTT1	TTC2	CTC2	TTT2	CTT2	TTC3	CTC3	TTT3	CTT3
H_1	7.65	8.09	7.97	8.54	7.64	8.12	7.97	8.62	7.67	8.14	7.99	8.65
H_2	9.52	9.09	7.45	7.04	9.51	9.00			9.55	9.02	7.51	
H_5	6.52		6.32		6.50		6.30	6.44	6.53		6.33	6.46
H_6	6.61		6.56						6.57			
H_7	6.87				6.82				6.82			
H_8	6.78				6.76							
H_9	6.65	6.84										
H_{10}	7.21	7.39	7.49		7.24	7.44	7.78		7.27	7.50	7.80	
$H_{2'}$	7.01	7.41	7.06			7.47				7.46		
$H_{3'}$		7.00	7.24									
$H_{2''}$	6.73	6.74		7.20	6.54				6.76	6.79		
$H_{3''}$	6.47			6.79	6.55				6.76			
$H_{4''}$	6.57											

Blanks correspond to non-measurable values due to overlapping; the chemical shifts of $H_{7''}$, $H_{8''}$ and $H_{9''}$ in open forms of NP2 and $H_{7''}$, $H_{8''}$, $H_{10''}$, $H_{11''}$ and $H_{12''}$ in open forms of NP3 were not distinguished due to overlapping.

been fully proved during analysis of data obtained from further kinetic analysis (see Section 3.2).

The set of chemical shifts determined for all of the three investigated compounds, substituted by one, two and three thienyl groups is reported in Table 1.

3.2. Kinetic analysis of the thermal relaxation after UV irradiation

After UV irradiation, ^{1}H NMR spectra were recorded at regular time intervals and at different temperatures between 218

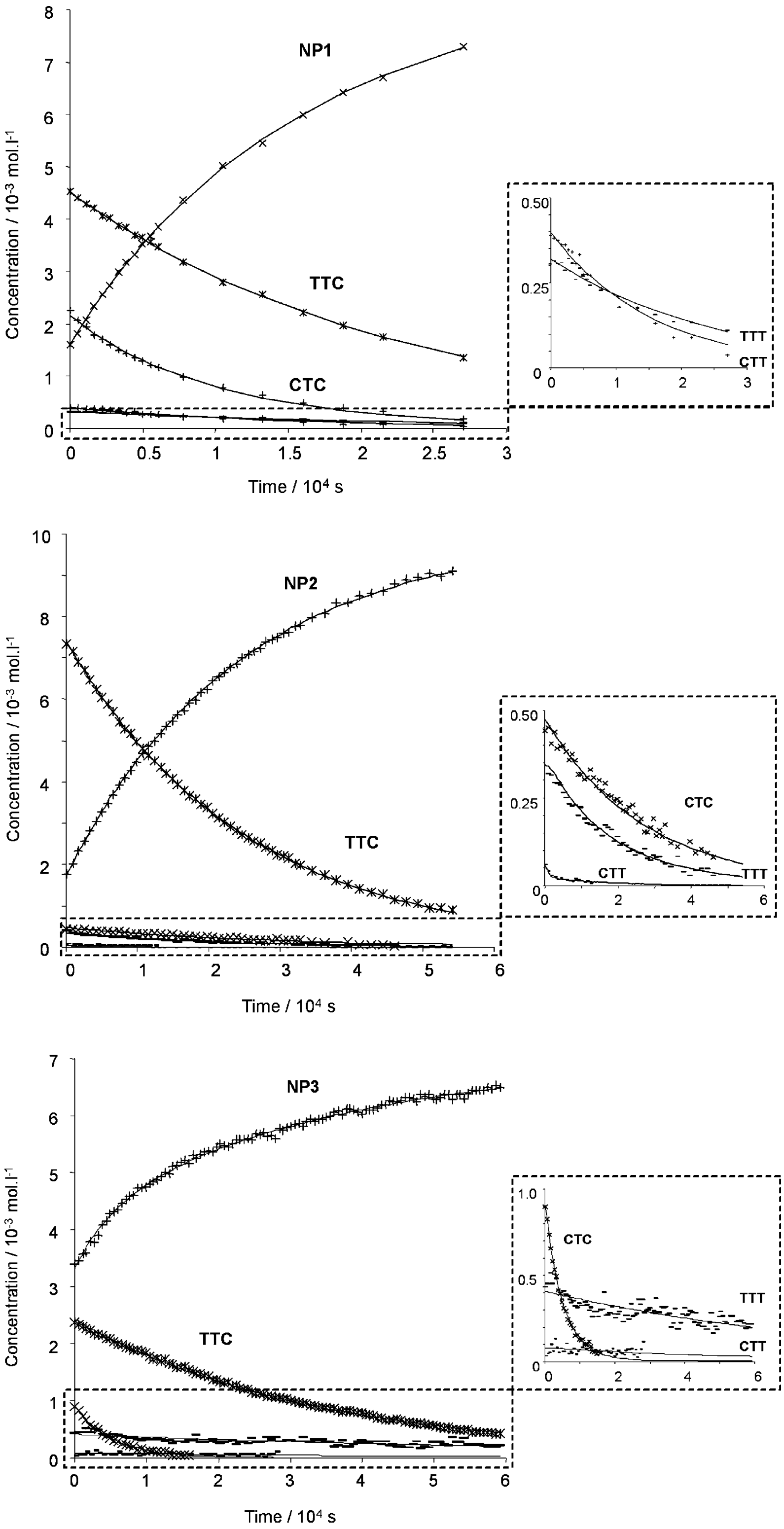

Fig. 4. Thermal relaxation of NP1, NP2 and NP3 at 233 K (starting time $t = 0$ corresponds to the end of the UV irradiation of the thermostated sample). Symbols are experimental data and continuous line fitting from the model (insets are magnification of the relaxation kinetics of the lower concentration isomers).

and 253 K. By measuring several specific NMR signals (H_2 in NP, H_2 in TTC and CTC and H_1 in CTT and TTT), the time-evolution of concentrations of the initial closed form and of the four photoproducts, TTC, CTC, TTT and CTT, can be plotted during the thermal relaxation in the dark (Fig. 4).

From our kinetic modelling approach using for each compound, the simultaneous fitting of the five kinetic curves, it was found for compound NP1 and NP3 that only four irreversible paths (among the putative sixteen as shown in Scheme 2) were sufficient to obtain a good fit between the experimental data points and the calculated kinetic curves (see Scheme 3). It must be pointed out that the data analysis has also confirmed the assignment of CTT and TTT. Indeed, the compound which decays towards TTC isomer corresponds to the signal at 7.97 ppm (i.e. to P4 = TTT) and that which decays towards CTC corresponds to signal at 8.54 ppm (i.e. to P3 = CTT). Surprisingly, some supplementary reverse processes (CTC → TTC, and possibly CTC → CTT and TTC → TTT) need to be considered to reproduce accurately all the relaxation kinetics of the bithienyl compound, NP2. It appears that such isomerisation processes must be taking into account during fitting procedure [26], but the low correlation coefficients in the corresponding Eyring's plot indicate that this observation is not completely ascertained.

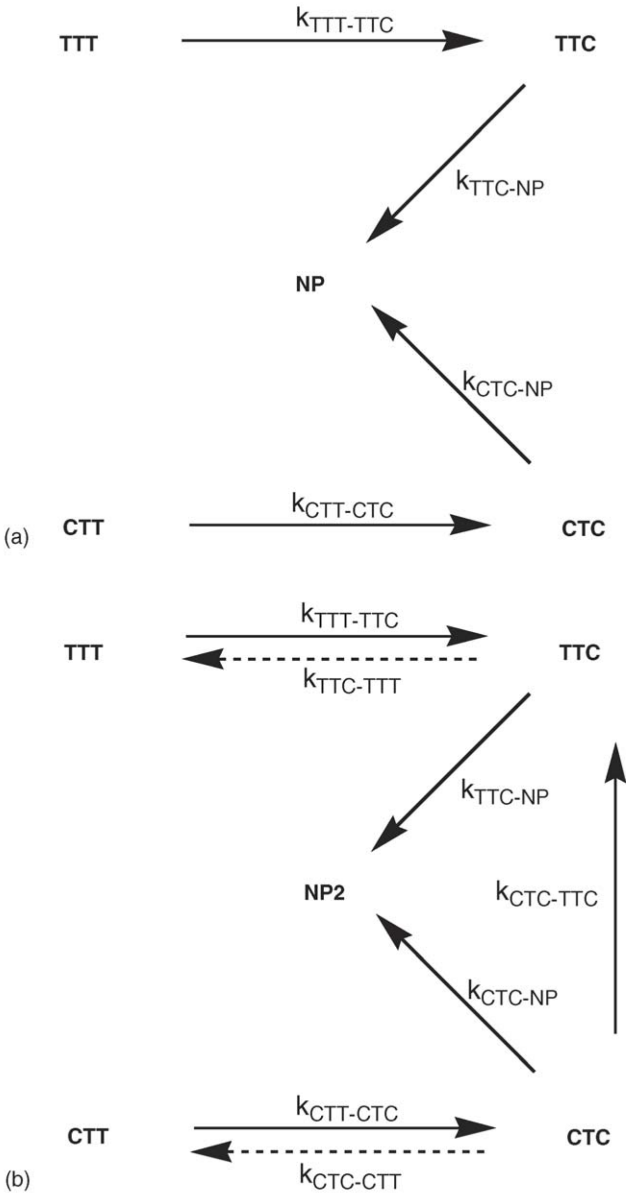

Scheme 3. Successive irreversible paths during the thermal relaxation in the dark recorded after UV irradiation of (a) compounds NP1 and NP3 and (b) compound NP2. Dotted arrows indicate possible but not fully confirmed paths.

By plotting $\ln(k_{i\to j}/T)$ versus $1/T$ at several temperatures ranging from 218 to 253 K, we obtained straight lines, thus verifying Eyring's equation:

$$\ln\left(\frac{k_{i\to j}}{T}\right) = \frac{-\Delta H^{\#}}{RT} + \frac{\Delta S^{\#}}{R} + \ln\left(\frac{k_{\mathrm{B}}}{h}\right)$$

with k_{B}, Boltzmann's constant = 1.38×10^{-23} J K^{-1}; h, Planck's constant = 6.626×10^{-34} J s and $R = 8.314$ J mol^{-1} K^{-1}.

From the slope and the intercept, the values of the enthalpy of activation $\Delta H^{\#}$ and of the entropy of activation $\Delta S^{\#}$ were calculated. Results are gathered in Table 2.

For the three compounds under investigation, among the ring closure processes, CTC → NP is faster than the corresponding TTC → NP. The respective activation parameters are given in Table 2. Among the rate constants of trans/cis isomerisation,the CTT → CTC is faster than the corresponding TTT → TTC with the following activation parameters: $41 < \Delta H^{\#} < 83.4$ kJ mol^{-1} and $-156.2 < \Delta S^{\#} < 32.1$ J mol^{-1} K^{-1}. These values are of the same order of magnitude than those previously reported for symmetrical compounds [19].

Our kinetic analysis shows that the ring closure towards the initial naphthopyran NP occurs from the TTC or the CTC isomer and that these isomers derive from their TTT and CTT homologues, respectively, and that there is no direct path from TTT and CTT isomers to NP. For compound NP2, the substitution in 3-position by a bithienyl group provides the possibility of the observation of the CTC → TTC process.

3.3. Kinetic analysis of photocolouration under UV irradiation

The photocolouration under UV irradiation was investigated at 218 K for all of the compounds. At this temperature, it is assumed that the thermal relaxation can be neglected. Each sample of NP1, NP2 and NP3 was irradiated during 20 min by period of 2 min. After each period, ^{1}H NMR spectrum has been recorded. By measuring peak intensities, the course of the photoisomerizations can be plotted (Fig. 5).

The kinetic curves of the concentration versus time were modelled using the five-species system (Scheme 2). We found good fits between experimental and calculated data by considering seven processes. The same mechanism has been deduced for the three naphthopyrans NP1, NP2 and NP3 (see Scheme 4). UV irradiation of the initial closed form leads irreversibly to transoid–cis type photomerocyanines TTC and CTC. Both are in photoequilibrium with their respective transoid–trans isomer, TTT and CTT. An irreversible photoconversion of CTC into

Table 2
Thermal rate constants (k_Δ in 10^{-5} s^{-1}) of the various pseudo-elementary relaxation processes

	218	223	228	233	238	243	248	253	$\Delta H^\#$	$\Delta S^\#$	r^2
TTC1 → NP1	0.39		2.30	4.72	10.9		34.3	89.5	67.4	−36.2	0.9967
CTC1 → NP1	0.88		5.13	11.4	22.7		91.2	231	69.5	−20.3	0.9981
TTT1 → TTC1	0.12		2.51	4.04	37.9		–	72.8	83.4	32.1	0.9013
CTT1 → CTC1	0.72		–	6.53	–		–	36.9	49.3	−113.3	0.9871
TTC2 → NP2	0.36	0.92	1.88	4.23		17.7	34.6		66.0	−43.5	0.9997
CTC2 → NP2	1.22	3.54	4.20	6.66		76.9	121		67.8	−26.7	0.9527
TTT2 → TTC2	–	0.76	1.41	3.72		14.5	26.9		65.1	−49.2	0.9969
CTT2 → CTC2	2.40	–	18.4	–		47.3	55.3		43.2	−129.5	0.9079
TTC2 → TTT2	0.42	–	–	0.14		1.03	–				a
CTC2 → TTC2	1.71	0.99	2.55	2.32		7.24	29.2		40.6	−152.7	0.7917
CTC2 → CTT2	–	6.33	3.20	5.90		0.37	–				a
TTC3 → NP3	0.28	0.69	1.51	3.22		15.0			67.7	−38.0	0.9996
CTC3 → NP3	1.77	4.19	11.7	19.4		47.7			56.4	−73.0	0.9707
TTT3 → TTC3	0.55	1.09	0.94	1.20		8.28			41.0	−156.2	0.8053
CTT3 → CTC3	0.26	–	4.73	–		34.0			82.5	31.9	0.9619

Activation parameters $\Delta H^\#$ (kJ mol^{-1}) and $\Delta S^\#$ (J mol^{-1} K^{-1}) calculated from the corresponding Eyring's plots; a, non-significant correlation; -, non-significant values which have been omitted.

TTC is also existing (Scheme 4). The set of the seven apparent photochemical rate constants (h_{ij}) is reported in Table 3.

Table 3 shows that the number of thiophene groups affects the colouration process as the half time of conversion increases regularly from 210 to 575 s going from NP1 to NP3. This sequence is confirmed if we also consider the diphenyl homologue NP0 ($t_{[\mathrm{NP}]0/2} = 150$ s, [19]). Such behaviour has already been observed and interpreted as a consequence of the decrease of the photochromic reactivity at the expense of the fluorescence quantum yield when the number of thienyl units increases [28]. For the same reason, the apparent photochemical rate constant ($h_{\mathrm{NP}\rightarrow\mathrm{CTC}}$) of the naphthopyran ring opening towards CTC (NP + $h\nu$ → CTC) is clearly decreasing. Another clear-cut effect with the number of thiophene units is the increase of the apparent direct and reverse photoisomerization rate constants between CTT and CTC ($h_{\mathrm{CTT}\rightarrow\mathrm{CTC}}$ and $h_{\mathrm{CTC}\rightarrow\mathrm{CTT}}$). These results are confirmed by the examination of the quantum yields ratio, which illustrates the peculiar role of the terthiophene derivative NP3. While the quantum yield ratio $\Phi_{\mathrm{NP}\rightarrow\mathrm{TTC}}/\Phi_{\mathrm{NP}\rightarrow\mathrm{CTC}}$ ranges between 0.5 and 0.7 for NP2 and

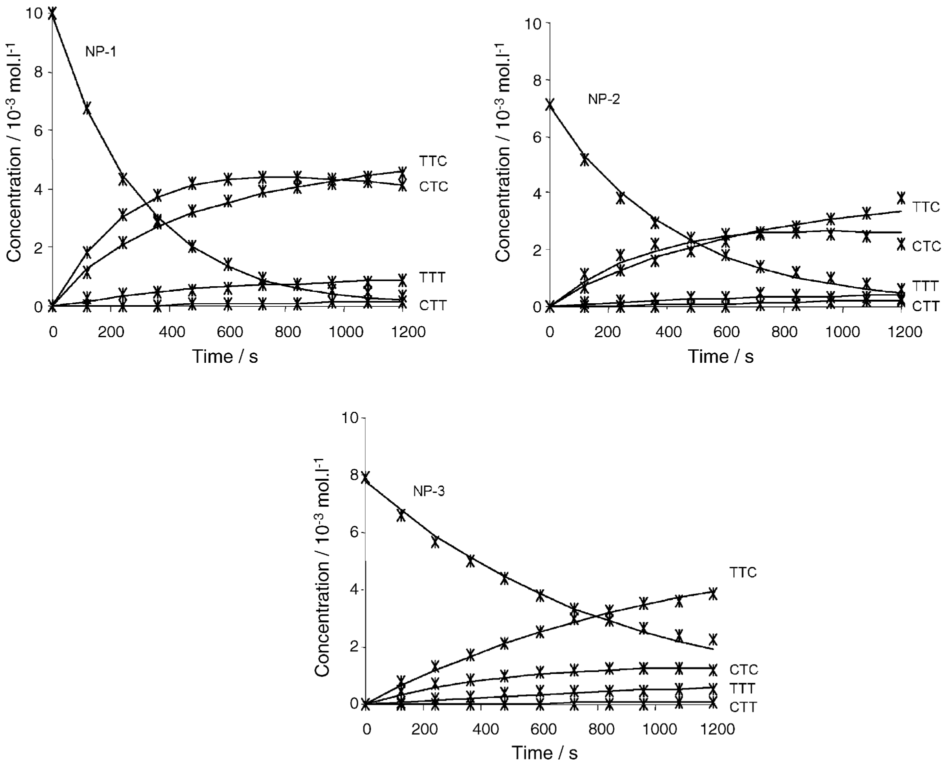

Fig. 5. Photocolouration process of three naphthopyrans at 218 K under UV irradiation (symbols are experimental concentrations; solid lines are best fits from our model).

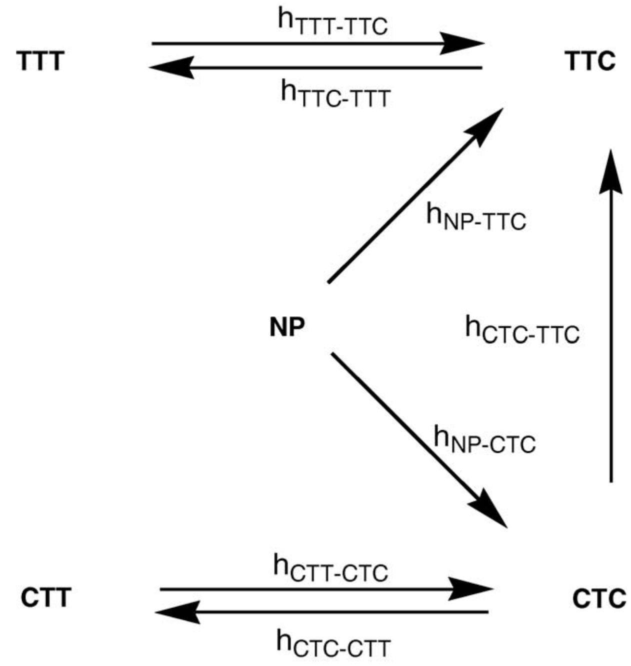

Scheme 4. Photoisomerization processes of the 3-thienyl naphthopyrans under UV irradiation.

NP1, respectively, it reaches 2.1 for NP3. Similarly, the quantum yield ratio $\Phi_{CTC \rightarrow TTC}/\Phi_{CTC \rightarrow CTT}$ ranges between 8.7 and 9.1 for NP1 and NP2, respectively, while it levelled at 4.9 for NP3. Finally, our results also show that the cis/trans isomerization photoequilibria TTT ← → TTC and CTT ← → CTC are both displaced towards the TC side thus strongly limiting the accumulation of CTT and TTT during the NP UV irradiation. However, these photoequilibria do not appear to be very sensitive to the number of thiophene units. The ratio of the photochemical apparent rate constants range from 0.12 to 0.19 and 0.11 to 0.37 for the two photoequilibria, respectively. Other processes involving the formation or isomerisation of the TTC isomer seem less sensitive to the influence of the number of thiophene units.

Table 3
Results from kinetic analysis of the photocolouration process at 218 K

	NP1	NP2	NP3
$t_{[NP]0/2}$	210 s	300 s	575 s
$t_{[CTC]max}$	720 s	720 s	840 s
$\%[CTC]_{max}$	44%	38%	13%
$\%[NP]_{end}$	2%	6%	19%
$\%[TTC]_{end}$	46%	48%	40%
$\%[CTC]_{end}$	42%	37%	13%
$\%[TTT]_{end}$	9%	6%	6%
$\%[CTT]_{end}$	1%	3%	1%
$h_{NP \rightarrow TTC}$	1.4×10^{-3}	0.8×10^{-3}	0.8×10^{-3}
$h_{NP \rightarrow CTC}$	1.9×10^{-3}	1.5×10^{-3}	0.4×10^{-3}
$h_{TTC \rightarrow TTT}$	3.5×10^{-3}	1.7×10^{-3}	2.9×10^{-3}
$h_{TTT \rightarrow TTC}$	18.1×10^{-3}	13.8×10^{-3}	19.1×10^{-3}
$h_{CTT \rightarrow CTC}$	1.9×10^{-4}	2.1×10^{-4}	8.7×10^{-4}
$h_{CTC \rightarrow CTT}$	3.5×10^{-5}	7.8×10^{-5}	10.0×10^{-5}
$h_{CTC \rightarrow TTC}$	3.1×10^{-4}	7.1×10^{-4}	4.9×10^{-4}
$\Phi_{NP \rightarrow TTC}/\Phi_{NP \rightarrow CTC}$	0.7	0.5	2.1
$\Phi_{CTC \rightarrow TTC}/\Phi_{CTC \rightarrow CTT}$	8.7	9.1	4.9
$h_{TTC \rightarrow TTT}/h_{TTT \rightarrow TTC}$	0.19	0.12	0.15
$h_{CTC \rightarrow CTT}/h_{CTT \rightarrow CTC}$	0.18	0.37	0.11

h_{ij}, apparent photochemical rate constant of process $i \rightarrow j = \Phi_{ij}\varepsilon_i l I_0 F$; Φ_{ij}/Φ_{ik}, ratio of the quantum yield of the $i \rightarrow j$ process to the quantum yield of the $i \rightarrow k$ process ($=h_{ij}/h_{ik}$); h_{ij}/h_{ji}, ratio of apparent photochemical rate constants for photoequilibrium $i \leftarrow \rightarrow j$; $t_{[NP]0/2}$, time of irradiation for half-conversion; $t_{[CTC]max}$, time of irradiation to reach $[CTC]_{max}$; $\%[X]_{max}$, ratio of concentrations at their optimum value; $\%[X]_{end}$, ratio of concentrations at the end of the UV irradiation period.

4. Conclusion

Three 3-phenyl-3H-naphtho[2,1-b]pyrans linked to one, two, or three thiophene units in 3 position of the pyran moiety by a covalent bond have been investigated by NMR spectroscopy under UV irradiation and during the thermal relaxation in the dark. In each case, the four transoid isomers of photomerocyanines have been characterized. The kinetic analysis of photocolouration and thermal relaxation processes made it possible to propose plausible mechanisms on the basis of time evolution of the concentrations. UV irradiation of NP produces directly TTC and CTC photomerocyanines, which are then reversibly photoisomerised to TTT and CTT. An unexpected photochemical pathway from CTC to TTC was also observed. Photochemical ring opening NP → CTC has been shown to be clearly sensitive to the number of thienyl units. The NP3 compound behaves differently, giving lower concentrations of photomerocyanines especially a significant diminution of the CTC isomer. The effect of the number of thienyl units is more difficult to see during the thermal relaxation. However, careful examination of the activation parameters of the CTC → NP path shows that NP3 exhibits the lower $\Delta H^{\#}$ and $\Delta S^{\#}$ values. It is likely that a larger number of thiophene increases the number of degrees of freedom making the ring closure energetically favoured but entropically unfavourable.

Acknowledgements

The 300 MHz NMR facilities were funded by the Région Nord-Pas de Calais (France), the Ministère de la Jeunesse, de l'Education Nationale et de la Recherche (MJENR) and the Fonds Européens de Développement Régional (FEDER). Part of this collaborative work was performed within the framework of the "Groupe de Recherche: Photochromes Organiques, Molécules, Mécanismes, Modèles", GDR CNRS no 2466.

References

[1] C. Moustrou, N. Rebière, A. Samat, R. Guglielmetti, A. Yassar, R. Dubest, J. Aubard, Helv. Chim. Acta 81 (1998) 1293–1301.
[2] M. Frigoli, C. Moustrou, A. Samat, R. Guglielmetti, Helv. Chim. Acta 83 (2000) 3043–3052.
[3] M. Frigoli, C. Moustrou, A. Samat, R. Guglielmetti, Eur. J. Org. Chem. (2003) 2799–2812.
[4] F. Garnier, G. Horowitz, X.Z. Peng, D. Fichou, Adv. Mater. 2 (1990) 592–594.
[5] G. Horowitz, X.Z. Peng, D. Fichou, F. Garnier, J. Mol. Electron. 7 (1991) 85–89.
[6] J. Roncali, Chem. Rev. 92 (1992) 711–738.
[7] A. Peters, N. Branda, Adv. Mater. Opt. Electron. 10 (2000) 245–249.

[8] K. Higashiguchi, K. Matsuda, M. Matsuo, T. Yamada, M. Irie, J. Photochem. Photobiol. A: Chem. 152 (2002) 141–146.

[9] T. Yamaguchi, Y. Fujita, H. Nakazumi, S. Kobatake, M. Irie, Tetrahedron 44 (2004) 9863–9869.

[10] S. Pu, T. Yang, J. Xu, L. Shen, G. Li, Q. Xiao, B. Chen, Tetrahedron 61 (2005) 6623–6629.

[11] K. Higashiguchi, K. Matsuda, Y. Asano, A. Murakami, S. Nakamura, M. Irie, Eur. J. Org. Chem. 1 (2005) 91–97.

[12] B. Moine, G. Buntinx, O. Poizat, M. Frigoli, C. Moustrou, A. Samat, Mol. Cryst. Liq. Cryst. 431 (2005) 363–368.

[13] N. Rebière, C. Moustrou, M. Meyer, A. Samat, R. Guglielmetti, J.C. Micheau, J. Aubard, J. Phys. Org. Chem. 13 (2000) 523–530.

[14] M. Frigoli, V. Pimienta, C. Moustrou, A. Samat, R. Guglielmetti, J. Aubard, F. Maurel, J.C. Micheau, Photochem. Photobiol. Sci. 2 (2003) 888–892.

[15] S. Xiao, T. Yi, F. Li, C. Huang, Tetrahedron Lett. 46 (2005) 9009–9012.

[16] V.Z. Shirinian, M.M. Krayushkin, D.M. Nikalin, A.A. Shimkin, O.Yu. Kuznetsova, A.V. Metelitsa, V.I. Minkin, Mol. Cryst. Liq. Cryst. 431 (2005) 329–335.

[17] F. Ortica, C. Moustrou, J. Berthet, G. Favaro, A. Samat, R. Guglielmetti, G. Vermeersch, U. Mazzucato, Photochem. Photobiol. 78 (2003) 558–566.

[18] F. Ortica, P. Smimmo, G. Favaro, U. Mazzucato, S. Delbaere, D. Venec, G. Vermeersch, M. Frigoli, C. Moustrou, A. Samat, Photochem. Photobiol. Sci. 3 (2004) 878–885.

[19] D. Venec, S. Delbaere, J.C. Micheau, M. Frigoli, C. Moustrou, A. Samat, G. Vermeersch, J. Photochem. Photobiol. A: Chem. 181 (2006) 174–179.

[20] S. Delbaere, J.C. Micheau, G. Vermeersch, J. Org. Chem. 68 (2003) 8968–8973.

[21] J. Berthet, J.-C. Micheau, A. Metelitsa, G. Vermeersch, S. Delbaere, J. Phys. Chem. A 108 (2004) 10934–10940.

[22] S. Delbaere, J.C. Micheau, M. Frigoli, G. Vermeersch, J. Org. Chem. 70 (2005) 5302–5304.

[23] M. Frigoli, Ph.D. thesis, Aix-Marseille II, 2000.

[24] K. Kaps, P. Rentrop, Comp. Chem. Eng. 8 (1984) 393–396;
M. Minoux, in: Dunod (Ed.), Programmation Mathematique, vol. 1, Bordas, Paris, 1983, pp. 95–168;
M.H. Deniel, D. Lavabre, J.C. Micheau, in: J.C. Crano, R.J. Guglielmetti (Eds.), Organic Photochromic and Thermodynamic Compounds, vol. 2, Plenum Press, New York, 1999, pp. 167–209.

[25] All the possible variations of the v_{ij} rate coefficients have been neglected. This assumption is fully justified if F is strictly constant. For instance, when the irradiation wavelength is close to an isobestic point or if the absorbance of the photochemical reacting solution is sufficiently low. As the irradiation light was not strictly monochromatic, Φ_{ij} and ε_i values must be considered as wavelength-averaged. Then, v_{ij} terms correspond to apparent first-order rate constants.

[26] The fitting procedure was always started using the full Scheme 2. It was then step by step reduced by removing all the non-necessary steps in order to obtain good fitting with the minimum number of isomerisation processes. It was also demonstrated that once a good fitting has been obtained, it was impossible to change the position of each selected pseudo-elementary reaction.

[27] S. Delbaere, B. Luccioni-Houze, C. Bochu, Y. Teral, M. Campredon, G. Vermeersch, J. Chem. Soc. Perkin Trans. 2 (1998) 1153–1157.

[28] A.E. Yassar, C. Moustrou, H. Youssoufi, A. Samat, R. Guglielmetti, F. Garnier, J. Chem. Soc. Chem. Commun. (1995) 471–472.